for the alkoxy radicals given above.

1,5-Exo cyclizations for radicals, including **2**, exhibit activation entropies in the range of −12 to −15 cal/(mol·K) (calculated from the data in Table II). The major contribution to this entropy change arises from the "freezing" of hindered rotations present in the open chain radical. The difference in the entropies of cyclopentane and pentene, 14.5 cal/(mol·K),[29] provides an estimate of the maximum expected contribution of 3.6 cal/(mol·K) per "frozen" rotation. As with the β-scission of **1**, the external rotational contribution is small, amounting to −0.66 cal/(mol·K) for the cyclization of **2** (see Table III).

Conclusions

The results presented above show that the β-scission of **1** is a reversible process in solution at temperatures from 6 to 80 °C.[37] They also provide absolute rate constants for the β-scission of **1** and the 1,5-exo cyclization of **2**. The reaction of *N*-alkoxypyridine-2-thiones with tributylstannane (**3**) has been shown to be a suitable system for the measurement of the rates of alkoxy radical reactions. With H• abstraction from **3** as a kinetic reference, the methods used in this study should allow the measurement of rate constants for a variety of alkoxy radical reactions within the range 10^6–10^9 s^{-1} for unimolecular processes and 10^4–10^9 M^{-1} s^{-1} for bimolecular processes.

Experimental Section

Materials and Analyses. All solvents were distilled prior to use. The purity of tributylstannane (**3**) was determined by H_2 evolution from its reaction with dichloroacetic acid. If the purity was below 95%, **3** was purified by vacuum distillation. Sodium pyridine-2-thione *N*-oxide was purified by precipitation from methanol/ethyl acetate and dried in vacuo to a constant weight (mp 276–279 °C, lit.[38] mp 285–290 °C). ^1H NMR spectra (200 MHz) were measured on a Varian XL-200 spectrometer. Analysis by gas chromatography was performed on a Varian 3400 with a 25-m phenyl methyl silicone capillary column; the response of the flame-ionization detector was calibrated with authentic compounds.

Preparation of *N*-(Cyclopentyloxy)pyridine-2-thione (6). The following manipulations were carried out with minimal exposure to light. Dry DMF (15 mL), sodium pyridine-2-thione *N*-oxide (1.5 g, 10 mmol), and cyclopentyl bromide (1.5 g, 10 mmol) were placed in a 50-mL round-bottom flask fitted with a reflux condenser. The contents were placed under argon and heated at 80 °C for 16 h. The dark yellow reaction mixture was diluted with 200 mL of 0.1 M aqueous NaOH and extracted with 5 × 50 mL aliquots of ether. The combined ether extracts were washed with 2 × 25 mL of H_2O and 25 mL of saturated NaCl and dried over $MgSO_4$. Removal of the solvent yielded an amber oil, which was further purified by column chromatography (ether, silica gel) to give **6** (0.6–0.8 g, 30–40%) as a yellow oil which eventually crystallized upon standing at −5 °C: mp 42–44 °C; MS, *m/z* 195.1; ^1H NMR ($CDCl_3$) δ 1.77 (m, 8 H), 5.62 (m, 1 H), 6.58 (dt, 1 H), 7.14 (dt, 1 H), 7.66 (m, 2 H). Anal. Calcd for $C_{10}H_{13}NOS$: C, 61.51; H, 6.71; N, 7.17. Found: C, 61.14; H, 7.04; N, 7.08.

Reactions of 6 with 3. Reactions were performed in Pyrex vials sealed with Teflon-surfaced rubber septa. In a typical experiment, a vial was wrapped in alumina foil and charged with 0.5 mL of a 0.030 M benzene solution at **6**. The vial was sealed, frozen in liquid nitrogen, evacuated, and filled with argon via a needle through the septum. The vial was then placed in a thermostated bath (±1 °C). After 15 min, **3** was injected through the septum to start the reaction. At temperatures ≥40 °C, the reactions were self-initiating and had gone to completion (yellow solutions became clear) within 1 h at 40 °C, 10 min at 60 °C, and 5 min at 80 °C. At temperatures <40 °C, the aluminum foil was removed after the addition of **3** and the reactions were initiated by exposure to a 250-W tungsten lamp and were complete within 5 min.

Registry No. 1, 53578-06-6; **2**, 78939-50-1; **6**, 114720-44-4; sodium pyridine-2-thione *N*-oxide, 15922-78-8; cyclopentyl bromide, 137-43-9; 5-bromo-1-pentanal, 1191-30-6.

(37) Independent studies in these laboratories of the cyclization of **2**, generated by the reaction of 5-bromo-1-pentanal with **3**, have confirmed the results presented in this paper.

(38) Barton, D. H. R.; Bridon, D.; Fernandez-Picot, I.; Zard, S. Z. *Tetrahedron* **1987**, *43*, 2733.

Diffusion–Reaction Kinetics Related to Grignard Reagent Formation. Analytic Steady-State Solution of a Simplified D Model, a Mechanism with First-Order Surface and First- and Second-Order Solution Steps[1]

John F. Garst,* Brian L. Swift, and Darwin W. Smith

Contribution from the Department of Chemistry, School of Chemical Sciences, The University of Georgia, Athens, Georgia 30602. *Received April 12, 1988*

Abstract: An analytic steady-state solution is obtained for a simplified "D model", a mechanism that may describe Grignard reagent formation. The reactive intermediate R is created at flux v at a planar solid surface. R and other intermediates Q and S diffuse freely in solution. R isomerizes to intermediate Q and reacts with the solvent SH, giving product RH and intermediate S. Q also reacts with solvent, giving QH and S. R, Q, and S react among themselves, giving products RR, RQ, RS, QQ, QS, and SS. At the surface, R, Q, and S react to form products RZ, QZ, and SZ. The transport of R, Q, and S is described by diffusion equations with the same coefficient D. The reactivities of R, Q, and S at the surface, with the solvent, and with one another are independent of the identity of the intermediate. Product yields vary with v and the parameters governing surface and solution reactivities of R, Q, and S. There is more isomerization in solution products than in those formed at the surface. Although a homogeneous reaction in either two or three dimensions would give a value of 2.0 for the yield ratio $Y_{RQ}/(Y_{RR}Y_{QQ})^{1/2}$, it is typically near 1.0 in the D model.

Kinetic treatments of the competitions that determine product distributions are essential tools for mechanistic investigations of reactions in homogeneous solutions. Similar studies have not been brought to bear on nonelectrochemical reactions that occur at liquid–solid interfaces, such as Grignard reagent formation. This may be for good reason; among the possible complications are the following. (1) Reaction conditions may be ill-defined or uncontrollable. (2) Reactants, intermediates, and products may adsorb on the surface of the solid. (3) Surfaces, concentrations,

(1) Based on: Swift, B. L. Ph.D. Dissertation, The University of Georgia, 1987.

0002-7863/89/1511-0234$01.50/0

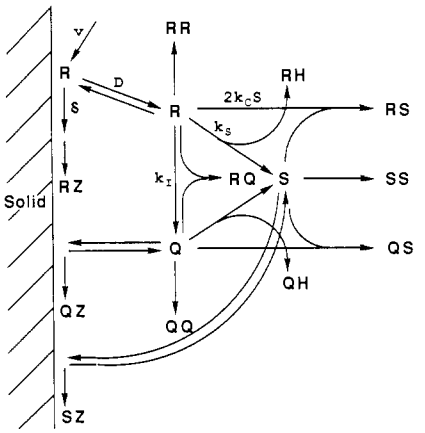

Figure 1. Processes included in the D model.

and temperatures may not be uniform. (4) Mass transport may occur through multiple and complex mechanisms, e.g., stirring, convection, boiling, diffusion.

Still, one may hope for simplicity. Idealized or approximate treatments might capture enough of the features of the actual situation to be useful. In another realm, there is a well-known example of a highly approximate but very useful treatment, Hückel molecular orbital theory.

We have solved analytically the steady-state kinetic equations for a simplified version of a reaction mechanism, the "D model", that may describe Grignard reagent formation. It includes first-order surface reaction steps and first- and second-order solution steps. Since it may apply to reactions other than Grignard reagent formation, the symbols used here for intermediates and products are generalized slightly.

We first describe the model. Then, we consider successively more complex cases, with brief discussions of some of the trends. Finally, we present figures that give results for the case of three reactive intermediates, one of which is formed at an insignificant level, and discuss the trends with parameter variation.

The solution of the equations of the simplified D model is outlined in the appendix. A BASIC computer program for the calculation is available as supplementary material.

In the following paper, calculations are compared with some available experimental data on Grignard reagent formation.[2]

Simplified D Model. "D" stands for "diffusion" and refers to the fact that reactive intermediates R, Q, and S diffuse freely in solution instead of being adsorbed at the surface. In the D model, the solid presents to the liquid a uniform plane surface ($x = 0$) of infinite extent. Intermediate R is formed in solution at a constant flux v in a plane parallel to and at a small distance s from the surface of the solid. R formation is distributed uniformly over the plane $x = s$. We treat the case in which the distance s approaches zero.

The reactions included in the D model are represented in Figure 1. In solution, R isomerizes to Q or reacts with solvent SH, forming RH and S. Q also reacts with solvent, forming QH and S. R, Q, and S undergo bimolecular reactions among themselves. Although the bimolecular reactions can be of any type, they are referred to here as "coupling" and the products are represented as RR, RQ, RS, QQ, QS, and SS. These solution reactions compete with surface reactions of R, Q, and S, which form products RZ, QZ, and SZ.

Isomerization of the initial intermediate R is included so that the analysis will apply to experiments using radical (or other) "clocks". An abbreviated form of the D model, omitting solution reactions other than isomerization, was described and discussed earlier.[3]

The following identities relate the D model to a possible mechanism of Grignard reagent formation. The solid is magnesium. R is an alkyl radical R• formed from alkyl halide RX in a reaction at the magnesium surface. Q is a radical Q• that results when R• isomerizes. S is a solvent-derived radical S• formed when R• or Q• abstracts a hydrogen atom from a solvent (usually an ether) molecule. RH and QH are the hydrocarbons that result from attack of R• and Q• on the solvent. RR, RQ, RS, QQ, QS, and SS are the products of bimolecular coupling or disproportionation among the radicals R•, Q•, and S•. RZ, QZ, and SZ are RMgX, QMgX, and the product(s) of reaction of S at the magnesium surface.

(2) Garst, J. F.; Swift, B. L. *J. Am. Chem. Soc.*, following paper in this issue.

(3) Garst, J. F.; Deutch, J. M.; Whitesides, G. M. *J. Am. Chem. Soc.* **1986**, *108*, 2490–2491.

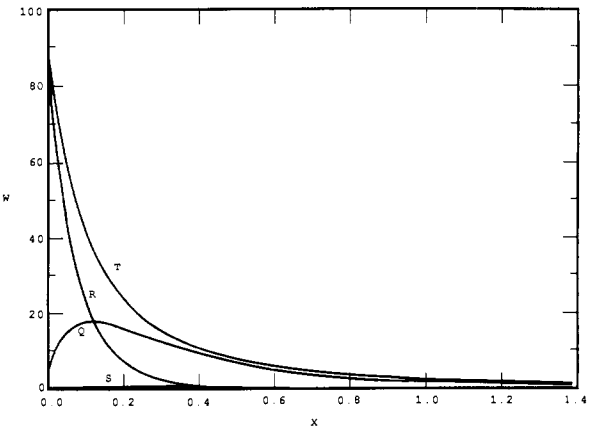

Figure 2. Steady-state concentration profiles for $V = 10^4$, $\Delta = 10^2$, and $G^2 = 10^2$. W is a dimensionless concentration (eq 6–8). X is the dimensionless distance from the surface of the solid (eq 5). If $2k_C = 3 \times 10^9$ M^{-1} s^{-1}, $k_I = 4.4 \times 10^5$ s^{-1}, and $D = 3 \times 10^{-5}$ cm^2 s^{-1}, then 100 on the W axis corresponds to 2.22×10^{-4} M and 1.0 on the X axis corresponds to 8216 Å.

Parameters. In the simplified D model, the intermediates R, Q, or S have the same diffusion coefficient D (cm^2 s^{-1}), the reactions of R and Q with solvent have the same rate constant k_S (s^{-1}), the reactions of R, Q, and S among themselves have the same (except for statistical factors) rate constant k_C (cm^3 mol^{-1} s^{-1}), and the reactions of R, Q, and S at the surface have the same reactivity parameter δ (cm^{-1}; see Appendix). The other parameters of the problem are the flux v (mol cm^{-2} s^{-1}) of the reaction that forms R at the surface and the rate constant k_I (s^{-1}) for the isomerization of R to Q.

To describe a particular physical case, values of the six parameters v, δ, D, k_I, k_S, and k_C are required. However, the problem actually has only three independent parameters. Scaling reduces the parameter set to the scaled reaction flux V (unscaled, v), the scaled surface reactivity Δ (unscaled, δ), and the scaled isomerization rate constant $G^2 - 1$ (unscaled, k_I), eq 1–3.

$$V = [4k_C/3(k_S{}^3D)^{1/2}]v \quad (1)$$

$$\Delta = (D/k_S)^{1/2}\delta \quad (2)$$

$$G^2 - 1 = k_I/k_S \quad (3)$$

Other quantities are scaled as in eq 4–8. Here t' and t are the scaled and unscaled time; X and x are the scaled and unscaled

$$t' = k_S t \quad (4)$$

$$X = (k_S/D)^{1/2}x \quad (5)$$

$$R = (4k_C/3k_S)[R] \quad (6)$$

$$Q = (4k_C/3k_S)[Q] \quad (7)$$

$$S = (4k_C/3k_S)[S] \quad (8)$$

distance from the surface; and R, Q, and S and [R], [Q], and [S] are the respective scaled and unscaled concentrations of intermediates R, Q, and S.

Since the system is heterogeneous, the steady-state concentrations R, Q, and S are functions of the distance X from the surface. Examples of calculated concentration profiles, for a set of parameters in the range appropriate for Grignard reagent formation from 5-hexenyl bromide, are given in Figure 2.

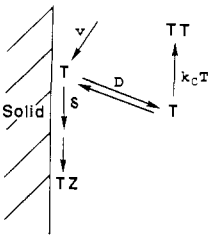

Figure 3. D model for an initial reactive intermediate T that couples but neither isomerizes nor reacts with solvent.

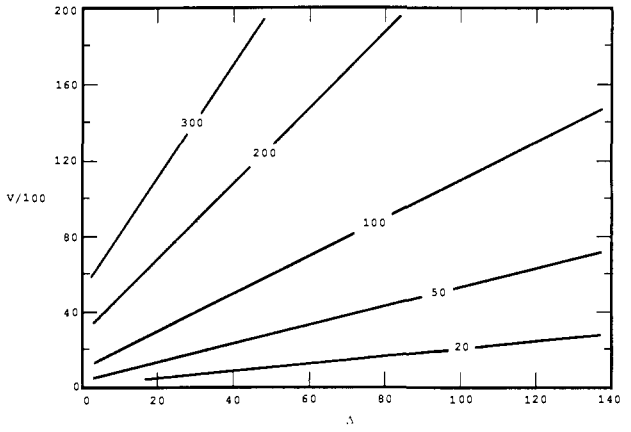

Figure 4. Total scaled concentration T_0 of intermediate(s) T at the surface of the solid.

T Case—Single Reactive Intermediate T, or T as the Sum of R, Q, and S. The reactions of intermediates can be divided into two groups, those in which net intermediates are destroyed (R → RZ, 2R → RR, Q → QZ, etc.) and those in which intermediates are merely interconverted (R → Q, R → S, Q → S). Since R, Q, and S have the same diffusion coefficient (D) and the same reactivity parameters (δ and k_C) for reactions in which net intermediates are destroyed, the sum T of R, Q, and S behaves exactly as would a single intermediate T that could only react at the surface and couple (Figure 3).

For this simple case, the steady-state concentration profile is given by eq 9, where T_0 is the scaled concentration of T at the

$$T = 4/(X + C)^2 \qquad C = 2/T_0^{1/2} \tag{9}$$

surface. T_0 is obtained from eq 10. The yield Y_{TZ} of TZ is given

$$\Delta T_0 + T_0^{3/2} = V \tag{10}$$

by eq 11. Since the only other product is TT, its yield Y_{TT} is

$$Y_{TZ}^3/(1 - Y_{TZ})^2 = F = \Delta^3/V = 3D^2\delta^3/4k_C v \tag{11}$$

given by eq 12.

$$Y_{TT} = 1 - Y_{TZ} \tag{12}$$

Figure 4 shows how T_0 is related to V and Δ. For Grignard reagent formation, 10^4 and 100 are typical values of V and Δ, respectively. These values give T_0 near 100, which corresponds (for typical values $D = 3 \times 10^{-5}$ cm^2 s^{-1}, $k_S = 4.4 \times 10^3$ s^{-1}, and $2k_C = 3 \times 10^9$ M^{-1} s^{-1}) to 2.2×10^{-4} M. This is an unusually high steady-state concentration for an alkyl radical intermediate in solution. Such high radical concentrations explain reactivity patterns in Grignard reagent formation that were hitherto regarded as anomalous.[2]

Figure 2 shows a concentration profile of T for the same parameter values. A notable feature is the distance from the surface that the profile extends. The concentration of T is still significant at 8000 Å. However, since the rate of TT formation at a particular distance from the surface is proportional to T^2, it is seen that the majority of the TT is formed within the first 1000 Å or so.

Figure 5 gives the yield of TZ as a function of F (Δ^3/V or $3D^2\delta^3/4k_C v$). Y_{TZ} increases as F increases, that is, with increasing D or δ or with decreasing k_C or v. The effects of k_C, v, and δ are

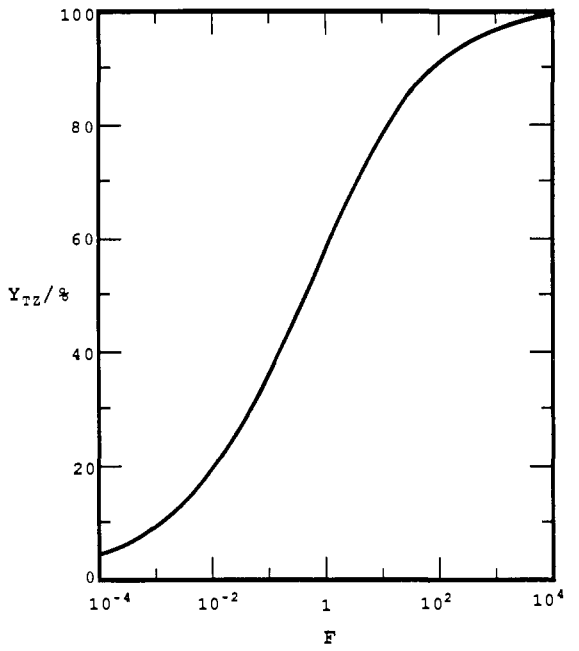

Figure 5. Yield Y_{TZ} of surface product TZ as a function of F (eq 11).

clearly the expected ones. Increased δ means increased reactivity in TZ formation; increased k_C means increased reactivity in coupling, which then competes better with TZ formation; and increased v results in higher steady-state concentrations of T, so that second-order coupling competes better with first-order TZ formation.

The effect of D (with other parameters constant) may be surprising, but it can be rationalized as follows. Diffusion trajectories, that is, the spatial paths followed by diffusing particles, are determined by time-independent factors. These trajectories are random walks (taken to the limit, for diffusion equations, of infinite step frequency and zero step size), meaning that after each diffusive step the direction of the next step is decided randomly.

Increasing the diffusion coefficient D does not change the trajectories; it simply increases the speed at which particles move along these trajectories. Thus, increasing D will decrease the mean lifetimes of intermediates T by increasing their frequencies of arrival at the surface and at collisions with other intermediates T, increasing the frequency of opportunities for reaction in both TZ and TT formation and therefore increasing the rate of T consumption. This decreases the steady-state concentration of T, which favors first-order TZ formation over second-order TT formation.

However, the net effect of changing D, taking into account the D dependencies of other parameters, is much more complex. If R (Figure 1) or T (Figure 3) production and coupling are diffusion-controlled (as in Grignard reagent formation), then $v = v^\circ D/D^\circ$ and $k_C = k_C^\circ D/D^\circ$, where the superscripts denote reference values. These D dependencies exactly cancel the D^2 in the numerator of F (eq 11). If there is no D dependence of δ, then the yield of TZ will be independent of D. But $\delta = b/D$, where $b = v_{TZ}/[T]_0$, v_{TZ}, being the flux of TZ formation. It seems possible that b itself could be D-dependent. Conceivably then, δ (and consequently the yield of TZ) could be independent of D.

In typical Grignard reagent preparations, yields are in the range 60–95%, corresponding to F values between 1 and 1000.

P Case—Intermediates P and S, or P as the Sum of R and Q. Since Q is formed from R, and since R and Q have identical diffusion coefficients and reactivities in corresponding reactions at the surface and with other intermediates, the sum P of R and Q behaves exactly as would a single intermediate P that could only undergo surface, solvent, and coupling reactions (Figure 6).

The equation for the steady state of P can be placed in a standard form (Riccati–Bessel) for which solutions are known. The solutions for the concentration profiles of P and S and for the yields of PZ, SZ, PP, PS, SS, and PH are much more complex

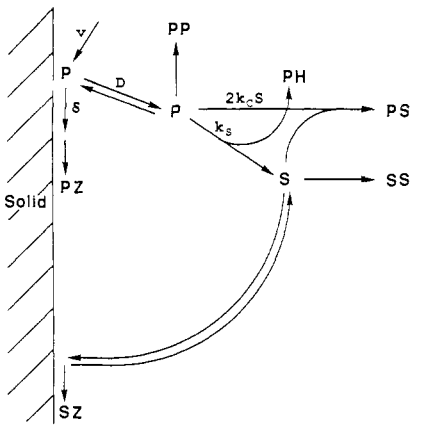

Figure 6. D model for an initial reactive intermediate P that couples and reacts with solvent but does not isomerize.

than for the T case (see Appendix).

In typical Grignard reagent preparations, there is very little reaction of alkyl radicals P with the solvent, so that S is everywhere very small, as illustrated in Figure 2. In such a case, the P profile is nearly coincident with that of T and the yields of PP and PZ are essentially those of TT and TZ.

R Case—Intermediates R, Q, and S. With solutions for T, P, and S in hand, only the solution for R remains, since Q is the difference P − R. Like the equation for P, the equation for R can be solved by placing it in Riccati–Bessel form.

Figure 2 gives the R, Q, and S profiles for parameter values in the range that is typically appropriate for Grignard reagent formation from 5-hexenyl bromide ($V = 10^4$, $\Delta = 10^2$, $G^2 = 10^2$). The negligible extent of solvent reaction for these parameters is reflected in the low profile of S; the P curve (not shown) is nearly coincident with the T curve. Only when k_S is increased by a factor of 100 (other unscaled parameters constant, giving $V = 10$, $\Delta = 10$) does attack of P on the solvent become very important ($Y_{PH} = 7\%$).

When the concentrations and distances of Figure 2 are unscaled with $2k_C = 3 \times 10^9$ M^{-1} s^{-1} (typical value for radical coupling), $k_1 = 4.4 \times 10^5$ s^{-1} (appropriate for the isomerization of the 5-hexenyl radical at 40 °C),[4] and $k_S = 4.4 \times 10^3$ s^{-1} (approximate for primary alkyl radical reactions with diethyl ether),[5] 100 on the scaled-concentration axis represents 2.2×10^{-4} M while 1.0 on the X axis represents ~8200 Å.

R is at its maximum value, corresponding to a concentration of $\sim 2 \times 10^{-4}$ M, at the surface. It dies away rapidly, having diminished to 10% of its surface value at a distance of ~1600 Å ($X = 0.2$). Q, however, increases initially with distance from the surface, reaching a maximum at 800–1000 Å (X near 0.1), after which it exceeds R and dies off much more slowly than R.

These trends are rational. Intermediates that are found at a great distance from the surface must have lived a relatively long time in order to reach that distance by diffusion. But the longer they have lived, the more probable it is that they have isomerized. Thus, the profile for R decreases while that for Q increases near the surface. With increasing distance from the surface, a higher proportion of T is Q. The Q profile turns down eventually because the T profile decreases continually with distance.

Inspection of Figure 2 reveals that RR, RQ, and QQ are preferentially formed at different distances from the surface. In a region sufficiently near the surface, most of the coupling gives RR. Farther from the surface, there is a region over which more RQ than RR or QQ is formed. Finally, at sufficient distances from the surface, most, then nearly all, of the coupling gives QQ.

Yield Functions I_{PZ}, I_{PP}, and H. Various functions of the product yields can be calculated in straightforward fashion. Of particular interest are the extents of isomerization in surface and solution products and the distribution among coupling products RR, RQ, and QQ.

The groups P in PZ are drawn from the steady-state pool of intermediates R and Q at the surface, but in PP they are drawn from the pool of intermediates that extends several thousand Ångstrom units into solution, over which concentrations vary. Consequently the extents of isomerization I_{PZ} and I_{PP}, that is, the fractions of Q in the groups P of PZ and PP, will differ. Since minimum isomerization in the steady-state pool of intermediates is at the surface, I_{PP} will be larger than I_{PZ}.

One measure of the distribution among the coupling products that constitute PP is the "homogeneity quotient" H (eq 13). For

$$H = Y_{RQ}/(Y_{RR}Y_{QQ})^{1/2} \tag{13}$$

homogeneous steady-state mass-action kinetics (in either two or three dimensions, $H = 2$ (eq 14). Since the concentrations of

$$H = 2k_C[R][Q]/[(k_C[R]^2)(k_C[Q]^2)]^{1/2} = 2 \text{ (homogeneous system)} \tag{14}$$

R and Q are not uniform in space in the D model, H can differ from 2.

Solvent Reaction. The yield of PH, which is a measure of the extent of reaction of intermediates P (R + Q) with the solvent, is determined by V and Δ only. This is easily seen from the fact that the yield of PH is obtained from solutions of the P case, for which V and Δ are the only parameters. G^2 is a parameter of the R case; it determines the proportioning of P between R and Q in the various products but has nothing to do with the extent of solvent reaction.

In figures below, we give calculated yields for ranges of V from 500 to 20 000 and of Δ from 0.5 to 140, all with $G^2 = 100$. Over this range of V and Δ, the yield of PH is small, as shown below.

The extent of solvent reaction decreases with increasing V and with increasing Δ. Increasing V results in a higher steady-state radical concentration, favoring second-order coupling with respect to first-order reactions with solvent. Increasing Δ favors surface products at the expense of solvent reaction and other solution products.

For $V = 500$ and $\Delta = 0.5$, the lower limits of the range we treat, the calculated yield of PH is 2.6%. Since increasing V or Δ or both leads to less solvent reaction, solvent reaction is practically negligible for the entire range with $V \geq 500$ and $\Delta \geq 0.5$.

Alternative Scaling for Negligible Solvent Reaction. Since solvent reaction is minor for our V–Δ range, it must be possible to express our results without reference to k_S. But k_S is a scale factor for time in our treatment (eq 4), and consequently, it enters the scaling of v, δ, and k_1 to V, Δ, and $G^2 - 1$ (eq 1–3). The alternative scaling described below eliminates k_S when solvent reaction is negligible.

If k_S were zero, then S would vanish, P and T would be equal, and k_S would not be available for use as a scale factor. Instead, k_1 could be used to scale time (replacing k_S in eq 4 and, where appropriate, others of eq 1–8). In that case a development parallel to that used here results in a system of two (instead of three) second-order differential equations that, with boundary conditions, are governed by only two independent parameters, V_1 and Δ_1 (eq 15 and 16), instead of the three that apply in the more general case.

$$V_1 = [4k_C/3(k_1^3 D)^{1/2}]v \tag{15}$$

$$\Delta_1 = (D/k_1)^{1/2}\delta \tag{16}$$

When k_S is nonzero but small enough that the reaction of P with solvent is only a minor perturbation on the other reactions, then V_1 and Δ_1 will be the only parameters affecting product distributions, to a good approximation. Eliminating k_S from eq 1–3 gives equations that, upon identification of V_1 and Δ_1, relate these quantitites to V, Δ, and $G^2 - 1$ (eq 17 and 18).

$$V = V_1(G^2 - 1)^{3/2} \tag{17}$$

$$\Delta = \Delta_1(G^2 - 1)^{1/2} \tag{18}$$

(4) Chatgilialoglu, C.; Ingold, K. U.; Scaiano, J. C. *J. Am. Chem. Soc.* **1980**, *102*, 5697–5699.

(5) The rate constant for reaction of the octyl radical with diethyl ether at 22 °C has been determined as 1.1×10^3 s^{-1}. Newcomb, M.; Kaplan, J. *Tetrahedron Lett.*, in press.

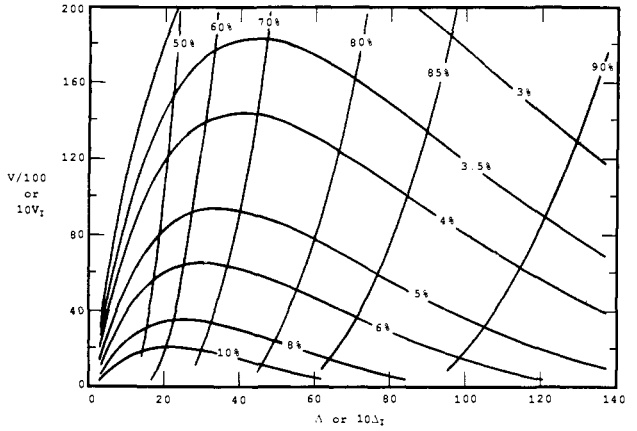

Figure 7. Yields of RZ (vertically tending lines) and QZ (horizontally tending lines) for $G^2 = 100$.

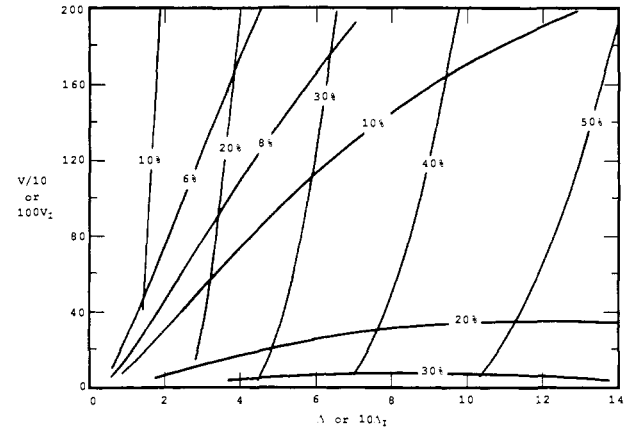

Figure 8. Enlargement of region near the origin of Figure 7.

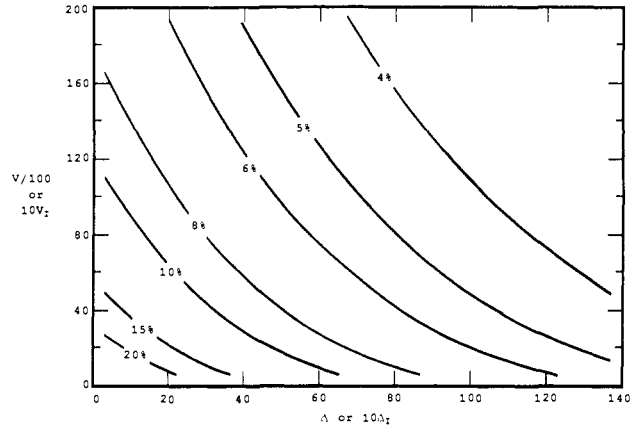

Figure 9. Extent I_{PZ} of isomerization in PZ for $G^2 = 100$.

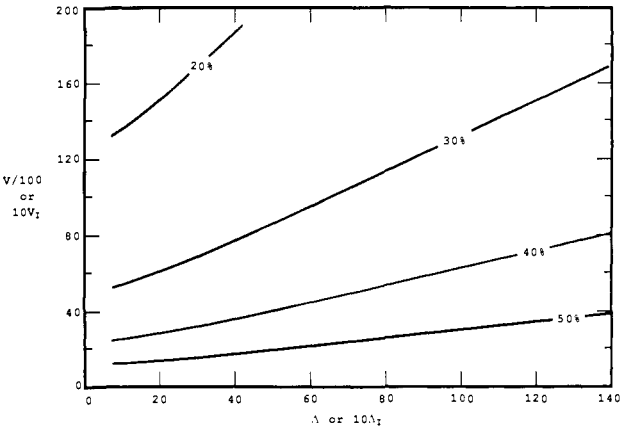

Figure 10. Extent I_{PP} of isomerization in PP for $G^2 = 100$.

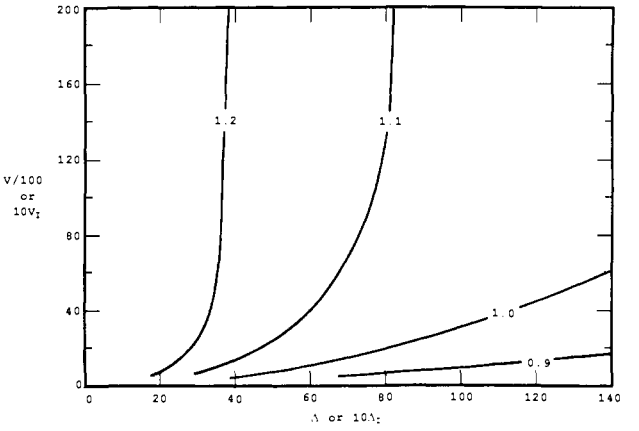

Figure 11. Homogeneity quotient H for $G^2 = 100$.

Results. Calculated yields for $V = 500$–$20\,000$, $\Delta = 0.5$–140, and $G^2 = 100$ are given in Figures 7–11. The value 100 for G^2 is appropriate, approximately, for 5-hexenyl as R ($k_I = 4.4 \times 10^5$ s^{-1} at 40 °C)[4] and diethyl ether as the solvent ($k_S = 4.4 \times 10^3$ s^{-1}).[5]

Since V_I and Δ_I alone will determine (to a good approximation) the product distributions for the range of parameter values considered here, we also give this alternative scaling of the axes of Figures 7–11. From eq 17 and 18, we find that $V = 985V_I$ and $\Delta = 9.95\Delta_I$ (for $G^2 = 100$). Thus, the axes of Figures 7–11 can be interpreted as V and Δ (with $G^2 = 100$) or as 10^3V_I and $10\Delta_I$ (to drawing accuracy).

The V_I–Δ_I interpretation of these figures is valid *only* when the reaction of P with solvent is negligible. It is valid then for *any* value of k_S. In most Grignard preparations, reactions with solvent occur only to a minor extent, so the two-parameter interpretation is appropriate.

The ranges plotted in Figures 7–11 cover some, but by no means all, of the parameter values that might be of interest in connection with Grignard reagent formation under various conditions. Thus, the figures are illustrative of trends, but they are not comprehensive in scope.

Yields are conveniently calculated by using a computer program. A BASIC program running under interpretation on a personal computer is adequate for this purpose. Such a program is provided as supplementary material.

Figures 7 and 8 give the yields of RZ and QZ as functions of V and Δ for $G^2 = 100$. The trends are rational. Increasing V at constant Δ will increase Y_{TT} (Figure 5) at the expense of Y_{RZ} and Y_{QZ}. Increasing Δ at constant V increases Y_{RZ} everywhere but increases Y_{QZ} only at low Δ values, decreasing it at higher values. The decreased Y_{TT} tends to increase both Y_{RZ} and Y_{QZ}, but the latter also tends to decrease because the lifetimes of intermediates are shortened, giving them less time for isomerization. The competing tendencies account for the observed trends.

Figures 9 and 10 show that the extents of isomerization I_{PZ} and I_{PP} in PZ and PP both decrease with increasing V at constant Δ. The intermediates have shorter lifetimes and less time for isomerization.

As Δ increases at constant V, I_{PZ} decreases; the intermediates that eventually become surface products have shorter lifetimes. But at the same time, I_{PP} increases. This is somewhat counterintuitive; a naive first thought might be that shorter lifetimes of the intermediates should decrease I_{PP} as they do I_{PZ}.

The increased I_{PP} can be explained in terms of diffusion trajectories. Some intermediates are on trajectories that take them to the surface frequently. As the surface reactivity Δ is increased, a higher fraction of these intermediates react, increasing the yield of the surface product PZ and decreasing that of PP. The intermediates with trajectories that lead to the surface less fre-

quently, however, are less susceptible to interception by reaction at the surface. The intermediates on these trajectories have a relatively high probability of isomerizing; they have long lifetimes before visiting the surface and having an opportunity to react there. They also have the best opportunities for coupling, since along their trajectories surface reactions do not complete effectively with coupling. Consequently, the effect of increasing Δ at constant V is to deplete the coupling product of contributions from shorter lived intermediates, leaving a larger relative contribution from intermediates with longer lifetimes, so that a larger fraction of those that do couple also isomerize.

Figure 11 shows the variation of the homogeneity quotient H with V and Δ for $G^2 = 100$. The most remarkable features are that, for the range of parameters that are plotted, all H values are significantly less than the "homogeneous kinetics" value of 2 and that H is remarkably insensitive to both V and Δ, varying only from 0.9 to 1.2 over most of the range.

Calculations. The calculations generating Figures 2, 4, and 7–11 were done by FORTRAN programs (VAX 750 computer) using numerical integrations (trapezoid rule) for yields of solution products. These and other calculations were checked by BASIC programs (Amiga 1000 computer) using Gauss quadrature and analytic integrations for yields of solution products.

Summary. The D model treated here is summarized in Figure 1. It is a plausible mechanism for the formation of Grignard reagents, and it also may apply to other reactions at liquid–solid interfaces.

The equations governing steady-state concentration profiles and competitive product formation are solved analytically.

Six rate parameters are required to describe the problem for a particular case: v, δ, D, k_C, k_I, and k_S (Figure 1). However, only three composite parameters survive after scaling. In our treatment, these are the scaled velocity V of R production, the scaled reactivity Δ of intermediates R, Q, and S at the surface, and the scaled isomerization rate constant $G^2 - 1$ (governing R $\rightarrow$ Q).

For parameters in the range appropriate to Grignard reagent formation from 5-hexenyl bromide, the T (scaled concentration of all intermediates, R + Q + S) extends significantly into solution to about X = 1, or ~8000 Å. R is dominant near the surface, but dies to insignificance at about $X = 0.3$, or ~2500 Å. Q increases with distance from the surface to a maximum near $X = 0.1$ (800–1000 Å) and decreases slowly thereafter. S is everywhere insignificant.

The yields of TZ (or PZ, when S formation is insignificant, where P = R + Q) and TT depend only on a single parameter, F, or $3D^2\delta^3/4k_Cv$. Y_{TZ} increases, and Y_{TT} decreases, with increasing F (Figure 5). The apparent D dependence of F, and therefore Y_{TZ}, disappears when k_C and v are proportional to D, leaving only δ as a possible D-dependent factor.

The relative rates of RZ and QZ production are proportional to the scaled surface concentrations R_0 and Q_0. Since R_0 is large and Q_0 small, RZ is heavily favored and the calculated extent of isomerization I_{PZ} in PZ (RZ + QZ) is small. However, the ratio R/Q decreases steadily with distance from the interface. Since most of the coupling occurs away from the surface, the extent of isomerization I_{PP} in coupling products is much greater than in PZ.

Coupling products RR, RQ, and QQ are formed in different proportions at different distances from the surface. Consequently, the quotient H $[Y_{RQ}/(Y_{RR}Y_{QQ})^{1/2}]$ deviates from the value of 2.0 that it would have under homogeneous conditions. It is near 1.0 over a wide range of parameters.

Although most of the calculated variations in product yields with changes in fundamental parameters governing diffusion and reactivity can be explained easily, a few appear to be counterintuitive at first glance. However, they can be rationalized by considering the nature of diffusion.

Acknowledgement is made to the donors of the Petroleum Research Fund, administered by the American Chemical Society, for support of this research. We are grateful to Professor G. S. Handler for helpful discussions and to Professor M. Newcomb for communicating pertinent results prior to publication.

Appendix

Analytic Solution of the Equations of the Simplified D Model. Mathematical Specification. We treat the steady state in the limit as s approaches zero. The equations to be satisfied are A1–A8.

$$D\,d^2[R]/dx^2 = (k_I + k_S)[R] + 2k_C([R]^2 + [R][Q] + [R][S]) \qquad x \neq s \tag{A1}$$

$$D\,d^2[Q]/dx^2 = -k_I[R] + k_S[Q] + 2k_C([R][Q] + [Q]^2 + [Q][S]) \tag{A2}$$

$$D\,d^2[S]/dx^2 = -k_S([R] + [Q]) + 2k_C([R][S] + [Q][S] + [S]^2) \tag{A3}$$

$$D[(d[R]/dx)_{s-} - (d[R]/dx)_{s+}] = v \tag{A4}$$

$$(d[R]/dx)_0 = \delta[R]_0 = (d[R]/dx)_{s-} = \delta[R]_s \qquad s \rightarrow 0 \tag{A5}$$

$$(d[Q]/dx)_0 = \delta[Q]_0 = \delta[Q]_s \qquad s \rightarrow 0 \tag{A6}$$

$$(d[S]/dx)_0 = \delta[S]_0 = \delta[S]_s \qquad s \rightarrow 0 \tag{A7}$$

$$\lim_{x\to\infty}[R] = \lim_{x\to\infty}[Q] = \lim_{x\to\infty}[S] = \lim_{x\to\infty}(d[R]/dx) = \lim_{x\to\infty}(d[Q]/dx) = \lim_{x\to\infty}(d[S]/dx) = 0 \tag{A8}$$

Equations A1–A3 describe the steady state. The left side of each equation is the rate of increase of [R], [Q], or [S] at x due to diffusion, while the right side is the rate of decrease due to chemical reaction. Equation A4 replaces eq A1 when $x = s$; it equates the net flux of R out of the plane $x = s$ in both directions (Fick's first law) to the production flux v of R in that plane. Equations A5–A7 express the radiation boundary condition,[6] which is appropriate for a surface that is partially absorbing (reacting) and partially reflecting toward species R, Q, and S. Equation A8 specifies boundary conditions at infinity.

The radiation boundary condition is equivalent to the assumption that the flux of an surface reaction is proportional to the concentration of the reactive intermediate at the surface. For example, the flux of RZ formation can be expressed as $b[R]_0$, where b is a constant of proportionality. By Fick's first law, the flux is also given by $D\,(d[R]/dx)_0$. Equating these two rate expressions gives $(d[R]/dx)_0 = (b/D)[R]_0$. The surface reactivity parameter δ is thereby identified as b/D.

Equalities involving $(d[R]/dx)_{s-}$ and $[R]_s$ appear in eq A5 because we treat the limit in which $s \rightarrow 0$. The derivative $d[R]/dx$ is discontinuous at $x = s$, where [R] has its maximum value.

Scaling to dimensionless parameters according to eq 1–8, gives eq A9–A16 from A1–A8.

$$d^2R/dX^2 = G^2R + (3/2)(R^2 + RQ + RS) \qquad x \neq s \tag{A9}$$

$$d^2Q/dX^2 = (1 - G^2)R + Q + (3/2)(RQ + Q^2 + QS) \tag{A10}$$

$$d^2S/dX^2 = -(R + Q) + (3/2)(RS + QS + S^2) \tag{A11}$$

$$(dR/dX)_{s-} - (dR/dX)_{s+} = V \tag{A12}$$

$$(dR/dX)_0 = \Delta R_0 = (dR/dX)_{s-} = \Delta R_s \qquad s \rightarrow 0 \tag{A13}$$

$$(dQ/dX)_0 = \Delta Q_0 = \Delta Q_s \qquad s \rightarrow 0 \tag{A14}$$

$$(dS/dX)_0 = \Delta S_0 = \Delta S_s \qquad s \rightarrow 0 \tag{A15}$$

$$\lim_{x\to\infty} R = \lim_{x\to\infty} Q = \lim_{x\to\infty} S = \lim_{x\to\infty}(dR/dX) = \lim_{x\to\infty}(dQ/dX) = \lim_{x\to\infty}(dS/dX) = 0 \tag{A16}$$

Since we treat the limit in which s approaches 0, we solve eq A9–A11 for concentration profiles only in the region $x \geq s$. In the following, R, Q, S, and related symbols represent scaled concentrations in this region of space only. Symbols such as R_0

(6) Rice, S. A. In *Comprehensive Chemical Kinetics*; Bamford, C. H., Tipper, C. H., Compton, R. G., Eds.; Elsevier: Amsterdam, 1985; Vol. 25.

represent the limit of R_s as s approaches zero.

Solution for T. Using T = R + Q + S, we obtain eq A17 as the sum of eq A9–A11. It is also the equation for the steady

$$d^2T/dX^2 = (3/2)T^2 \quad (A17)$$

state for the mechanism of Figure 3. Letting Z be dT/dX allows eq A17 to be replaced by A18 and A19, the quotient of which

$$dZ/dX = (3/2)T^2 \quad (A18)$$

$$dT/dX = Z \quad (A19)$$

is eq A20, which integrates to eq A21. The constant of integration

$$dZ/dT = (3/2)(T^2/Z) \quad (A20)$$

$$dT/dX = -T^{3/2} \quad (A21)$$

is zero because Z and T approach zero as X approaches infinity. Since dT/dX must be negative for $x > s$, the negative square root of T^3 is required.

Integration of eq A21 gives eq 9. The constant C is evaluated at $x = s$ in the limit as s approaches zero. Here T_0 is yet to be determined.

$$T = 4/(X + C)^2 \qquad C = 2/T_0^{1/2} \quad (9)$$

Defining Y_{TZ} (yield of TZ) as the fraction of the intermediates R (Figure 1) or T (Figure 3) that are converted to TZ, we express Y_{TZ} in terms of Δ and T_0. Equation A22 follows from eq A12

$$(dT/dX)_{s-} - (dT/dX)_{s+} = V \quad (A22)$$

and the facts that dQ/dX and dS/dX, but not dR/dX, are continuous at $x = s$. In the limit as s approaches zero, $(dT/dX)_{s-}$ approaches $(dT/dX)_0$, the scaled flux of formation of TZ, which can also be written as ΔT_0 (sum of eq A13–A15). Substituting ΔT_0 for $(dT/dX)_{s-}$ and $-T_0^{3/2}$ for $(dT/dX)_{s+}$ (eq A21) gives eq 10. Since ΔT_0 and V are the fluxes of formation of TZ and R,

$$\Delta T_0 + T_0^{3/2} = V \quad (10)$$

respectively, Y_{TZ} is given by eq A23. Eliminating T_0 from eq

$$Y_{TZ} = \Delta T_0/V = (V - T_0^{3/2})/V = 1 - 8/C^3V \quad (A23)$$

10 and A23 gives eq 11, which is solved for Y_{TZ}, so that both T_0

$$Y_{TZ}^3/(1 - Y_{TZ})^2 = F = \Delta^3/V = 3D^2\delta^3/4k_C v \quad (11)$$

(eq A23) and C (eq 9) are obtained, allowing the computation of the concentration profile of T. Since TZ and TT are the only products, Y_{TT} (yield of TT, fraction of R or T consumed in TT formation) is simply $1 - Y_{TZ}$ (eq 12).

$$Y_{TT} = 1 - Y_{TZ} \quad (12)$$

Solution for P. Equation A24 is both the sum of eq A9 and

$$d^2P/dX^2 = P + (3/2)PT \quad (A24)$$

A10 (P = R + Q; T = P + S) and the corresponding equation for the mechanism of Figure 6. Defining U (eq A25) and substituting $4/U^2$ for T (eq 9) gives eq A26.

$$U = X + C \quad (A25)$$

$$d^2P/dU^2 = [1 + 6/U^2]P \quad (A26)$$

This equation is placed in Riccati–Bessel form by the substitution $z = iU$ (eq A27).[7] The general solution is eq A28, where

$$z^2(d^2P/dz^2) + (z^2 - 6)P = 0 \qquad z = iU \quad (A27)$$

$$P = A'zj_2(z) + Bzy_2(z) \quad (A28)$$

A' and B are constants and $j_2(z)$ and $y_2(z)$ are independent spherical Bessel functions (eq A29 and A30).[7]

$$zj_2(z) = (3z^{-2} - 1)\sin(z) - 3z^{-1}\cos(z) \quad (A29)$$

$$zy_2(z) = -3z^{-1}\sin(z) - (3z^{-2} - 1)\cos(z) \quad (A30)$$

Replacing z with iU and the resulting trigonometric functions with their hyperbolic equivalents gives eq A31. Since P must

$$P = (A'/i)[(3/U^2 + 1)\sinh(U) - (3/U)\cosh(U)] + B[(3/U^2 + 1)\cosh(U) - (3/U)\sinh(U)] \quad (A31)$$

be real, A' must be imaginary or zero. Let $A = A'/i$, where A is real, and replace cosh (U) by its equivalent exp($-U$) + sinh (U). Equation A32 results. The outer boundary condition, that P

$$P = (3/U^2 + 1)[B\exp(-U) + (B - A)\sinh(U)] + (3/U)[A\exp(-U) - (B - A)\sinh(U)] \quad (A32)$$

approaches zero as U (or X) approaches infinity, requires that $A = B$, eq A33–A35. In eq A35, P_0 and M_0 are the limits of

$$P = B\exp(-U)(U^2 + 3U + 3)/U^2 = BM \quad (A33)$$

$$M = \exp(-U)(U^2 + 3U + 3)/U^2 \quad (A34)$$

$$B = P_0/M_0 \quad (A35)$$

P_s and M_s as s approaches zero.

Equation A36 is an analogue of eq A22. Eq A37 follows from eq A33 by taking the derivative. Equations A13 and A14, A34

$$(dP/dX)_{s-} - (dP/dX)_{s+} = V \quad (A36)$$

$$(dP/dX) = (dP/dU) = -B\exp(-U)[U^3 + 3U^2 + 6U + 6]/U^3 \quad (A37)$$

and A35, and A37 and the fact that $U_0 = C$ (eq A25) provide eq A38. The yield Y_{PZ} of PZ (RZ + QZ) is given by eq A39.

$$P_0 = VC/[\Delta C + (C^3 + 3C^2 + 6C + 6)/(C^2 + 3C + 3)] \quad (A38)$$

$$Y_{PZ} = \Delta P_0/V \quad (A39)$$

Thus, P_0 and Y_{PZ} can be calculated from Δ and V. They are independent, as they must be, of $G^2 - 1$, the scaled value of k_1. The yield of SZ is given by eq A40.

$$Y_{SZ} = Y_{TZ} - Y_{PZ} \quad (A40)$$

Solution for R. The solution for R is precisely parallel to that for P. Defining u (eq A41 and A42) and substituting $4G^2/u^2$ for

$$u = G(X + C) = GU \quad (A41)$$

$$u_0 = GC \quad (A42)$$

T (eq 9) in eq A9 gives eq A43, which is identical in form with

$$d^2R/du^2 = [1 + 6/u^2]R \quad (A43)$$

eq A26 with R and u of eq A43 corresponding to P and U of eq A26. Equations A44–A46, analogues of eq A33–A35, express

$$R = A\exp(-u)(u^2 + 3u + 3)/u^2 = AN \quad (A44)$$

$$N = \exp(-u)(u^2 + 3u + 3)/u^2 \quad (A45)$$

$$A = R_0/N_0 \quad (A46)$$

the solution in terms of R_0, the limit of R_s as s approaches zero. Equations A47–A50 are analogues of eq A37–A40.

$$(dR/dX) = G(dR/du) = -GA\exp(-u)[u^3 + 3u^2 + 6u + 6]/u^3 \quad (A47)$$

$$R_0 = VC/[\Delta C + (u_0^3 + 3u_0^2 + 6u_0 + 6)/(u_0^2 + 3u_0 + 3)] \quad (A48)$$

$$Y_{RZ} = \Delta R_0/V \quad (A49)$$

$$Y_{QZ} = Y_{PZ} - Y_{RZ} \quad (A50)$$

Yields of Solution Products. The yields of solution products are related to the integrals I of functions of T, P, and R from X

(7) Riccati-Bessel functions: Abramowitz, M.; Stegun, I. A. *Handbook of Mathematical Functions*; Dover: New York, 1965; Section 10.3, p 445. Originally published (1964) by the National Bureau of Standards; eighth Dover printing conforming to the tenth (December, 1972) printing by the Government Printing Office with some additional corrections.

= 0 to infinity (eq A51-A58), where T, P, and R are given by eq 9, A33, and A44.

$$I(\mathrm{P}) = \int_0^\infty \mathrm{P}\, \mathrm{d}X \quad \text{(A51)}$$

$$I(R) = \int_0^\infty \mathrm{R}\, \mathrm{d}X \quad \text{(A52)}$$

$$I(\mathrm{TT}) = \int_0^\infty \mathrm{T}^2\, \mathrm{d}X \quad \text{(A53)}$$

$$I(\mathrm{PT}) = \int_0^\infty \mathrm{PT}\, \mathrm{d}X \quad \text{(A54)}$$

$$I(\mathrm{RT}) = \int_0^\infty \mathrm{RT}\, \mathrm{d}X \quad \text{(A55)}$$

$$I(\mathrm{PP}) = \int_0^\infty \mathrm{P}^2\, \mathrm{d}X \quad \text{(A56)}$$

$$I(\mathrm{RP}) = \int_0^\infty \mathrm{RP}\, \mathrm{d}X \quad \text{(A57)}$$

$$I(\mathrm{RR}) = \int_0^\infty \mathrm{R}^2\, \mathrm{d}X \quad \text{(A58)}$$

For the integrations of eq A51-A58, we have used both numeric (trapezoid rule and Gauss quadrature from X = 0-20 with analytic integrations of the remaining tails, which have very small magnitudes, to infinity) and analytic methods, with agreement among them. Equations A59-A66 give the results of analytic integrations.

$$I(\mathrm{P}) = B[(3/C)E_2(C) + 3E_1(C) + e^{-C}] \quad \text{(A59)}$$

$$I(\mathrm{R}) = (A/G)[(3/GC)E_2(GC) + 3E_1(GC) + e^{-GC}] \quad \text{(A60)}$$

$$I(\mathrm{T}^2) = 16/3C^3 \quad \text{(A61)}$$

$$I(\mathrm{PT}) = (4B/C)[(3/C^2)E_4(C) + (3/C)E_3(C) + E_2(C)] \quad \text{(A62)}$$

$$I(\mathrm{RT}) = (4A/C)[(3/G^2C^2)E_4(GC) + (3/GC)E_3(GC) + E_2(GC)] \quad \text{(A63)}$$

$$I(\mathrm{P}^2) = \mathrm{B}^2[(9/C^3)E_4(2C) + (18/C^2)E_3(2C) + (15/C)E_2(2C) + 6E_1(2C) + e^{-2C}/2] \quad \text{(A64)}$$

$$I(\mathrm{RP}) = AB[(9/G^2C^3)E_4[(G+1)C] + [9(G+1)/G^2C^2]E_3[(G+1)C] + [3(G^2+3G+1)/G^2C]E_2[(G+1)C] + [3(G+1)/G]E_1[(G+1)C] + e^{-(G+1)C}/(G+1)] \quad \text{(A65)}$$

$$I(\mathrm{R}^2) = (A^2/G)[(9/G^3C^3)E_4(2GC) + (18/G^2C^2)E_3(2GC) + (15/GC)E_2(2GC) + 6E_1(2GC) + e^{-2GC}/2] \quad \text{(A66)}$$

$$\int_a^\infty e^{-by}\, \mathrm{d}y/y^n = a^{-(n-1)} \int_1^\infty e^{-abt} dt/t^n = a^{-(n-1)}E_n(ab) \quad \text{(A67)}$$

Here the $E_n(z)$ are exponential integrals (A67) that are described, for example, by Abramowitz and Stegun, who also tabulate their values and give accurate numerical approximations.[8] Except for a multiplicative constant, each term of each integrand of eq A51-A58 (when expressed as a function of U) is of the form of eq A67.

The fluxes of formation of solution products, corresponding to the mass-action terms for product formation in eq A9-A11, are given by combinations of these integrals, taking into account the relationships among T, P, R, Q, and S. The yield of each product is the formation flux divided by V, the flux of formation of R (eq A68-A75).

$$Y_{\mathrm{PH}} = I(\mathrm{P})/V \quad \text{(A68)}$$

$$Y_{\mathrm{RH}} = I(\mathrm{R})/V \quad \text{(A69)}$$

$$Y_{\mathrm{QH}} = [I(\mathrm{P}) - I(\mathrm{R})]/V \quad \text{(A70)}$$

$$Y_{\mathrm{TT}} = (3/2)I(\mathrm{T}^2)/V = 8/C^3V \quad \text{(compare eq 12)} \quad \text{(A71)}$$

$$Y_{\mathrm{PP}} = (3/2)I(\mathrm{P}^2)/V \quad \text{(A72)}$$

$$Y_{\mathrm{PS}} = 3[I(\mathrm{PT}) - I(\mathrm{P}^2)]/V \quad \text{(A73)}$$

$$Y_{\mathrm{SS}} = (3/2)[I(\mathrm{T}^2) + I(\mathrm{P}^2) - 2I(\mathrm{PT})]/V \quad \text{(A74)}$$

$$Y_{\mathrm{RR}} = (3/2)I(\mathrm{R}^2)/V \quad \text{(A75)}$$

$$Y_{\mathrm{RQ}} = 3[I(\mathrm{RP}) - I(\mathrm{R}^2)]/V \quad \text{(A76)}$$

$$Y_{\mathrm{QQ}} = (3/2)[I(\mathrm{P}^2) + I(\mathrm{R}^2) - 2I(\mathrm{RP})]/V \quad \text{(A77)}$$

$$Y_{\mathrm{RS}} = 3[I(\mathrm{RT}) - I(\mathrm{RP})]/V \quad \text{(A78)}$$

$$Y_{\mathrm{QS}} = 3[I(\mathrm{PT}) + I(\mathrm{RP}) - I(\mathrm{P}^2) - I(\mathrm{RT})]/V \quad \text{(A79)}$$

Registry No. Mg, 7439-95-4.

Supplementary Material Available: A listing of a computer program for calculating product yields and concentration profiles [in interpreted BASIC, a double-precision (16 decimal digits) calculation takes ~3 s on an Amiga 1000] (14 pages). Ordering information is given on any current masthead page.

(8) Exponential integral: Reference 7; Chapter 5, pp 227-251.

Mechanism of Grignard Reagent Formation. Comparisons of D-Model Calculations with Experimental Product Yields[1]

John F. Garst* and Brian L. Swift

Contribution from the Department of Chemistry, School of Chemical Sciences, The University of Georgia, Athens, Georgia 30602. *Received April 12, 1988*

Abstract: For the reaction of 5-hexenyl bromide in diethyl ether with magnesium at 40 °C, calculations based on a mechanism (the D model) in which intermediate alkyl radicals diffuse freely agree in detail and within probable experimental error with the product distribution reported by Bodewitz, Blomberg, and Bickelhaupt (*Tetrahedron* **1975**, *31*, 1053). All parameters of the calculation are taken or estimated from independent experiments. When the net rate and the reactivities of alkyl radicals at the magnesium surface are adjusted for best fit, the agreement is also excellent for solvent THF and good to excellent for solvents and solvent mixtures involving di-*n*-butyl and di-*n*-pentyl ethers and benzene, as well as diethyl ether, THF, and benzene.

According to Kharasch and Reinmuth,[2] "it might be said that he who knows and understands the Grignard reactions has a fair grasp of organic chemistry, for most fundamental processes have prototypes or analogs in phenomena observable in Grignard

0002-7863/89/1511-0241$01.50/0